Structure, Vol. 12, 2113–2124, December, 2004, ©2004 Elsevier Ltd. All rights reserved. DOI 10.1016/j.str.2004.09.020

Membrane Protein Crystallization in Lipidic Mesophases with Tailored Bilayers

Lisa V. Misquitta,[1] Yohann Misquitta,[2] Vadim Cherezov,[1] Orla Slattery,[1,5] Jakkam M. Mohan,[1] David Hart,[1] Mariya Zhalnina,[4] William A. Cramer,[4] and Martin Caffrey[1,2,3,5,*]

[1]Department of Chemistry
[2]Biophysics Program
[3]Biochemistry Program
The Ohio State University
Columbus, Ohio 43210
[4]Department of Biological Sciences
Purdue University
West Lafayette, Indiana 47907
[5]College of Science
University of Limerick
Limerick
Ireland

Summary

Monoacylglycerols have been used as bilayered hosts for growing crystals of membrane proteins. To date, the lipids used have had chains 16 and 18 carbon atoms long. We hypothesized that a shorter-chained lipid producing a thinner bilayer would facilitate the so-called in meso crystallization process. A 14 carbon monoacylglycerol was chosen as the lipid with which to test the proposal. To be compatible with the in meso method, a *cis* olefinic bond was placed in its acyl chain at a location arrived at by rational design. The target lipid was synthesized and was shown to form the requisite mesophase at room temperature. In support of the hypothesis, it produced crystals of bacteriorhodopsin and the outer membrane transporter, BtuB. The latter is the first β barrel protein to be crystallized by the in meso method. Protein stability in the short-chain lipid and how this relates to crystallogenesis are discussed.

Introduction

Eight years ago, the so-called "cubic phase" or "in meso" method for crystallizing membrane proteins was introduced (Landau and Rosenbusch, 1996). The method cut its teeth on the light-driven proton pump, bacteriorhodopsin (bR), an integral membrane protein that had resisted crystallographic attempts on its high-resolution structure determination for decades (Luecke et al., 1998). With the announcement of this radically new approach to membrane protein crystallogenesis that made use of lipidic mesophases, expectations ran high. In the intervening period, the method has been used successfully for high-resolution structure determination studies on several photocycle intermediates of bR (Lanyi and Schobert, 2004), halorhodopsin (Kolbe et al., 2000), sensory rhodopsin II (SRII) (Luecke et al., 2001), an SRII/transducer complex (Gordeliy et al., 2002), and the photosynthetic reaction center from *Rhodobacter sphaeroides* (Katona et al., 2003). The highest-resolution structure reported for the in meso method is that of the K intermediate of bR (1.43 Å) (Schobert et al., 2002). Other membrane proteins have produced crystals or microcrystals by the in meso method that diffract poorly or do not diffract at all. These include the acetylcholine-bungarotoxin complex (Paas et al., 2003), the reaction center from *Blastochloris* (formerly *Rhodopseudomonas*) *viridis* (Chiu et al., 2000), and the light-harvesting 2 complex from *Rhodopseudomonas acidophila* (LH2; Caffrey, 2003; Chiu et al., 2000). To put the method in perspective, of a total of 276 integral membrane protein entries in the PDB, 36 are attributed to the in meso approach (www.rcsb.org).

This level of output might be considered unimpressive given the time involved, and the method runs the risk of being dismissed as an "also-ran" and not a really useful tool for the membrane structural biologist. It is true that only four entirely new structures have been solved by using the in meso method, and all are, or include, rhodopsins of one form or another. While the reaction center represents a very different protein family, its structure was already available to high resolution, having been solved by the well-established vapor diffusion method (Stowell et al., 1997). Thus, the sense is that the in meso method may have limited range and that it is useful only with proteins consisting of compact transmembranal helical bundles stabilized by chromophores. Added to this less than stellar productivity is the *perceived* practical difficulty with all aspects of the in meso method. These problems range from having to work with highly viscous, sticky lipidic dispersions to difficulties seeing and harvesting crystals, particularly if the protein is not colored.

Some of the practical problems associated with the method have been solved. Recently, a relatively inexpensive robot has been introduced that can perform high-throughput in meso trials with just 20 nl of protein solution per screen (Cherezov et al., 2004). As will be shown in the current study (vide infra), and discussed elsewhere (Caffrey, 2003), while small, colorless crystals are a problem for any method, they can be handled by the in meso method with a little practice.

So, what about the yield of new protein structures? The view is that with the introduction of user-friendly tools that facilitate the in meso screening process, more proteins will be examined and a better measure of the method will be forthcoming. This represents work in progress.

There is also the issue of the hosting lipid that is integral to the in meso method and that will surely impact on its success. The original approach was developed by using monoolein (9.9 MAG; the monoacylglycerol [MAG] chain shorthand notation used here is based on the N.T system introduced previously (Misquitta and Caffrey, 2001). In this system, "N" refers to the neck of the chain extending from, and including, the carbonyl carbon to

*Correspondence: martin.caffrey@ul.ie

the first carbon of the *cis* olefinic bond. "T" refers to the tail of the chain extending from, and including, the second olefinic carbon to the carbon of the methyl terminus. The sum of N + T is the total number of carbon atoms in the chain. Thus, 9.9 MAG is monoolein that has an acyl chain that is 18 carbon atoms long and a *cis* double bond between carbons 9 and 10.). Just one other MAG, namely, monovaccenin (11.7 MAG), has been used successfully in in meso structure determination work (Gordeliy et al., 2002), while monopalmitolein (9.7 MAG) (Landau and Rosenbusch, 1996) and 7.9 MAG (Misquitta et al., 2004) have been reported to support crystallization of the benchmark integral membrane protein, bR.

We hypothesized that a shorter-chained MAG, if it formed the cubic phase under in meso conditions, would be a worthy candidate for in meso crystallogenesis for the following reasons. The low productivity of the in meso method with the three currently enlisted lipids may relate to the "degree of comfort" experienced by the protein in the bilayer of the hosting cubic phase membrane. Thus, with MAGs bearing chains that are 16 and 18 carbon atoms long, the bilayer accommodates the transmembranal protein to the point at which the driving force favoring protein-protein interaction and stable nucleus formation is not great. Obviously, it is strong enough because crystals do form in such environments. But, perhaps the driving force would be greater and would lead to better-quality crystals and to different crystal forms forming more rapidly with a shorter-chained lipid. In this case, mismatch between the hosting bilayer and the protein would not be so great as to trigger aggregation and unfolding, but it would be sufficient to enhance favorable protein-protein interactions and ultimately improved crystal growth.

In the current study, we set out to test this proposal. Before proceeding, however, we were mindful that the dictum "structure dictates function" also applies to lipids. The implication, therefore, was that the molecular structure of the lipid can profoundly impact its function at the level of mesophase behavior (tendency to form one or other of the liquid crystalline phases, Figure 1) and microstructure (bilayer thickness, water pore dimensions, etc.). Thus, the question of whether a shorter-chained MAG will form the requisite cubic phase under in meso conditions, including excess aqueous medium and room temperatures (19°C–25°C), arose?

For purposes of the current study, we decided that a MAG with an acyl chain that is 14 carbon atoms long would be short enough, but not too short. If the acyl chain had too few carbons, the protein would likely not reconstitute, which is considered to be a critical first step in the overall crystallogenesis process (Caffrey, 2000). However, the saturated C_{14} MAG variant, monomyristin, is a solid at room temperature and is unsuitable (Bailey, 1950; Lutton, 1965). Therefore, a *cis* double bond was called for to lower its melting temperature and to stabilize the cubic phase. It was not clear, however, as to where in the chain the olefinic bond should be placed. At this juncture, we invoked our accumulated knowledge of MAG phase behavior (Briggs, 1994; Briggs and Caffrey, 1994a, 1994b; Briggs et al., 1996; Chung and Caffrey, 1995; Misquitta and Caffrey, 2001; Misquitta et al., 2004; Qiu, 1998; Qiu and Caffrey, 1998, 1999, 2000) and our recently introduced "rational design" approach (Misquitta and Caffrey, 2001; Misquitta et al., 2004) to identify 7.7 MAG, with the double bond at carbon number 7, as being likely to have the desired properties. Importantly, 7.7 MAG was also expected to have phase properties significantly different from the routinely used 9.9 MAG, and it was these differences that gave rise to the expectation that it would prove useful as an alternative, perhaps an even better, system for crystallizing membrane proteins.

As described herein, 7.7 MAG has been rationally designed, synthesized, and purified. Its lyotropic (water-dependent) and thermotropic (temperature-dependent) phase properties, characterized by X-ray diffraction and polarized light microscopy (PLM), show that it formed the required cubic phase under in meso conditions. Accordingly, it was enlisted in in meso crystallization trials and produced bR crystals that were bigger and of better visual quality than those grown in the reference lipid, 9.9 MAG. True to expectation, 7.7 MAG-grown crystals were of diffraction quality and were in a different space group than those grown with 9.9 MAG. In addition, the new lipid system has produced crystals of the *E. coli* outer membrane cobalamin transporter, BtuB, that diffract to 4 Å. This is an important result because it is the first report of in meso crystal growth of an integral protein that crosses the membrane not as a compact helix bundle, but as a β barrel (Chimento et al., 2003). Furthermore, the protein is colorless, demonstrating that work with such proteins by the in meso method is indeed possible. As expected, 7.7 MAG supported crystal growth of the water-soluble protein, lysozyme, by the in meso method.

Results

Rational Design of Mesophase Behavior

By way of explaining how rational design works in the present context, we begin by introducing what has proven for us to be a useful way of considering how the different MAG homologs are related. This takes the form of what is called the N-T matrix (Figure 2B). Here, a given lipid is assigned a coordinate in N-T space as dictated by the length of the chain on either side of the olefinic bond (Figure 2A).

The target lipid in this study, 7.7 MAG, is represented in the N-T notation by N = 7 and T = 7 (yellow square in Figure 2B). Also included in Figure 2B is a series of MAGs for which detailed temperature-composition phase diagrams have been published. Three of these represent "N homologs" of 7.7 MAG in which N varies from 9 to 11, while T remains constant at a value of 7 (phase diagrams are surrounded by a bold line in Figure 2B). A perusal of these phase diagrams suggested that the N = 7 homolog, with the *cis* double bond at carbon atom number 7, has the correct chain length and would likely have the desired phase behavior. In turn, they were used to forecast the phase diagram for 7.7 MAG.

For each member of the homologous series represented in Figure 2B, the transition temperatures and compositions, at two and three phase coexistence re-

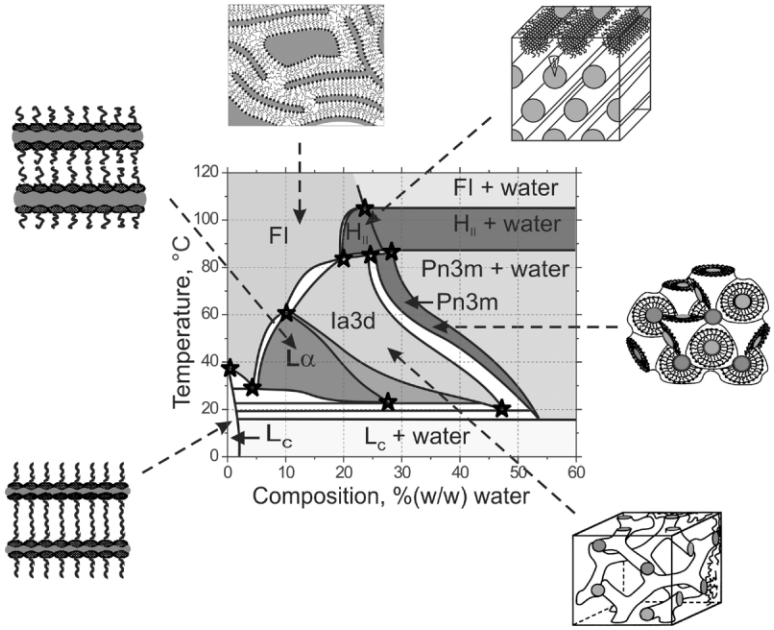

Figure 1. Stability and Structure of the Phases Formed by the 11.7 MAG/Water System

Stars identify critical coordinates used in predicting the phase diagram for the 7.7 MAG/water system (Figure 3). The figure has been redrawn from Qiu and Caffrey (1998). Cartoon representations of the various solid (lamellar crystal, Lc, phase), mesophase (lamellar liquid crystal, L_α, phase; cubic-Pn3m phase [space group number 224]; cubic Ia3d phase [space group number 230]; inverted hexagonal, H_{II}, phase), and liquid (fluid isotropic, Fl, phase) states are included.

gions, have been extracted from their respective phase diagrams. An example of how these transition values were obtained in the case of the 11.7 MAG/water system is shown in Figure 1. The corresponding transition temperatures have been plotted in Figure 3A as a function of N. Assuming that they are locally linearly related to N, the temperature expected for the various transitions undergone by 7.7 MAG were obtained by extrapolation (Figure 3A). A similar approach was taken for the major lyotropic transitions (Figure 3B). The predicted transition temperatures and compositions were placed in a blank phase diagram (stars in Figure 3C) and were used to construct a predicted diagram in accordance with established phase diagrams for other members of the homologous series, as described above.

A perusal of the phase diagram for 7.7 MAG (Figure 3C) shows that the required cubic phase is predicted to form under full-hydration conditions at slightly above 30°C. Accordingly, the relevant transition is a little on the high side given the intent to perform crystallization trials at room temperature (19°C–25°C). However, we chose to persevere with 7.7 MAG since the predicted transition temperature has an estimated error of ±5°C. This meant that the actual transition might well take place in the required temperature range. Furthermore, the predicted phase diagram for 7.7 MAG is dominated by the lamellar liquid crystal (L_α) phase. According to the proposed crystallization mechanism (Caffrey, 2000), a local lamellar structure acts as a conduit between the bulk cubic phase reservoir and the face of the crystal. Thus, the propensity of the short-chained lipid to form the L_α phase was considered a bonus.

Experimental Temperature-Composition Phase Diagram

Given the natural tendency of lipid/water phases to undercool (Qiu and Caffrey, 2000), we sought to obviate possible nonequilibrium behavior by collecting phase data in the heating direction. The phase diagram was constructed in the heating direction, and samples were initially incubated at −70°C for at least 3 hr in order to access the equilibrium solid, or Lc, phase. Phases were identified and structurally characterized by using low- and wide-angle X-ray diffraction (Supplemental Figure S1; available in the Supplemental Data online) and PLM (Supplemental Figure S2). Most of the diffraction measurements were made at discrete points in temperature-composition space. These are identified in Figure 4A as individual datum. This figure shows the actual phases identified by static diffraction measurements. Phase boundaries, positioned by using these data, are shown in Figure 4C. For ease of comparison, the data in Figure 4A and the interpreted phase diagram in Figure 4C are combined in Figure 4B. The excess water boundaries were located by using data for phase structure parameter dependence on sample water content of the type shown in Figure 5B at 10°C.

In addition to establishing the lyotropic (water-dependent) and thermotropic (temperature-dependent) phase properties of the 7.7 MAG/water system shown in Figure 5, the data therein show clearly that the desired, fully hydrated cubic phase forms in the vicinity of room temperature. This result was important, as it meant that it was appropriate to proceed with the in meso crystallization trials as planned.

7.7 MAG Supports Growth of Diffraction-Quality Crystals

Before using 7.7 MAG in in meso crystallization trials, the necessary control measurements were performed by using 9.9 MAG (monoolein), upon which the in meso method was based. The results illustrated in Figures 6A and 6B demonstrate that the latter supports the crystallization of the model membrane protein, bR, at 20°C, as expected. In this figure, crystals of bR of hexagonal habit are seen to grow to dimensions of ~80 × 80 × 10

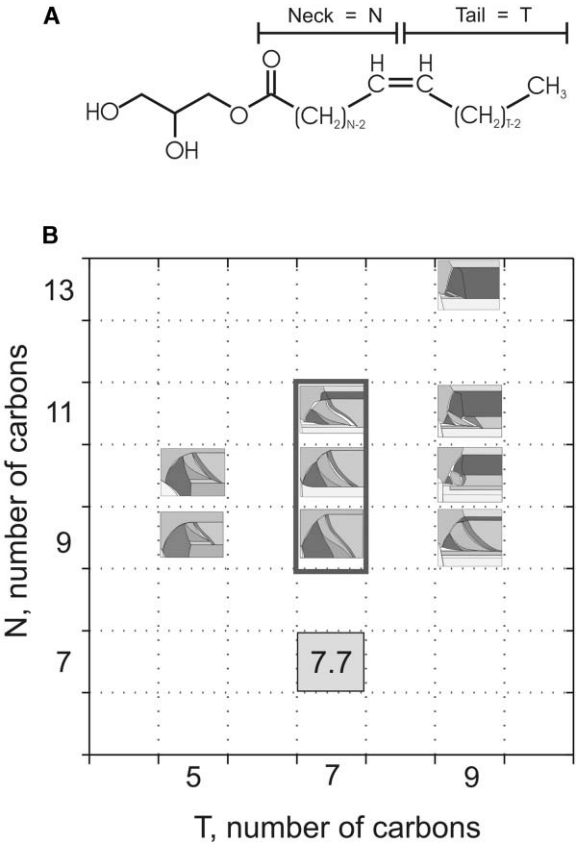

Figure 2. MAG Molecular Structure and Phase Behavior

(A) The molecular structure of the MAGs in the homologous series examined in this study. The carbons comprising the neck (N) and tail (T) portions of the acyl chains are indicated.

(B) The N-T matrix consisting of thumbnails of phase diagrams for homologous *cis*-monounsaturated MAGs. The square, bottom center, marked 7.7 represents the matrix location of the target lipid, 7.7 MAG. All phase diagrams are shown without detail. However, an expanded version of the phase diagram for the 11.7 MAG is shown in Figure 1. Thumbnails have been redrawn from published phase diagrams (9.7 and 10.7 MAGs: Briggs [1994]; 10.5 MAG: Briggs and Caffrey [1994a]; 9.5 MAG: Briggs and Caffrey [1994b]; 10.9 MAG: Misquitta and Caffrey [2001]; 11.9 MAG: Qiu [1998]; 11.7 MAG: Qiu and Caffrey [1998], 13.9 MAG, Qiu and Caffrey [1999]; 9.9 MAG: Qiu and Caffrey [2000]).

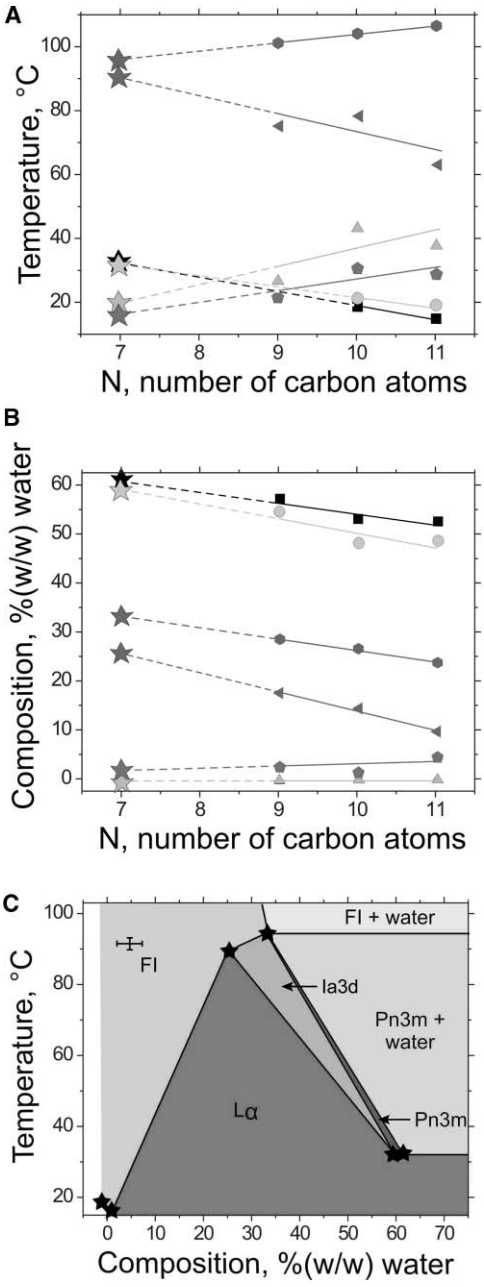

Figure 3. Predicting the Phase Transition Temperatures and Compositions of the 7.7 MAG/Water System from the Phase Behavior of Homologous MAGs

(A and B) (A) Phase transition temperatures and (B) phase transition compositions are plotted as a function of N. The phase transitions are identified as follows: triangle pointing up, Lc-to-Fl; pentagon, (Lc + L_α)-to-Fl; hexagon, liquid crystalline-to-Fl; square, Pn3m-to-(Pn3m + water); circle, L_α-to-(L_α + Ia3d); triangle pointing to the left, L_α-to-Ia3d. The solid lines are linear fits to the 9.7, 10.7, and 11.7 MAG data. The predicted transition values are marked by stars and were obtained by linear extrapolation from the known values.

(C) The predicted temperature-composition phase diagram for the 7.7 MAG/water system. The predicted transition points are indicated by stars and were obtained from data in (A) and (B). For simplicity, the phase boundaries have been drawn as straight lines. Estimated error bars are shown.

μm^3. These same conditions were used in turn to test 7.7 MAG as an in meso lipidic host for bR crystallization, also at 20°C. The data illustrated in Figures 6C and 6D show clearly that it serves well in this capacity. 7.7 MAG-grown crystals are larger (the maximum dimension recorded was 200 μm) than those observed with the reference 9.9 MAG. The crystals shown in Figures 6C and 6D have a maximum dimension in the range of 80–100 μm.

The above observations were made by using homemade crystallization plates designed for screening (Cherezov et al., 2004). Having thus identified conditions that supported crystal growth, the crystallization trials were repeated at 20°C by using plates that were more conducive to crystal harvesting. Crystals of bR that had been grown in 7.7 MAG were harvested, cryo-cooled, and used in crystallographic measurements. They were found to diffract to 2.1 Å in space group $C222_1$ (lattice

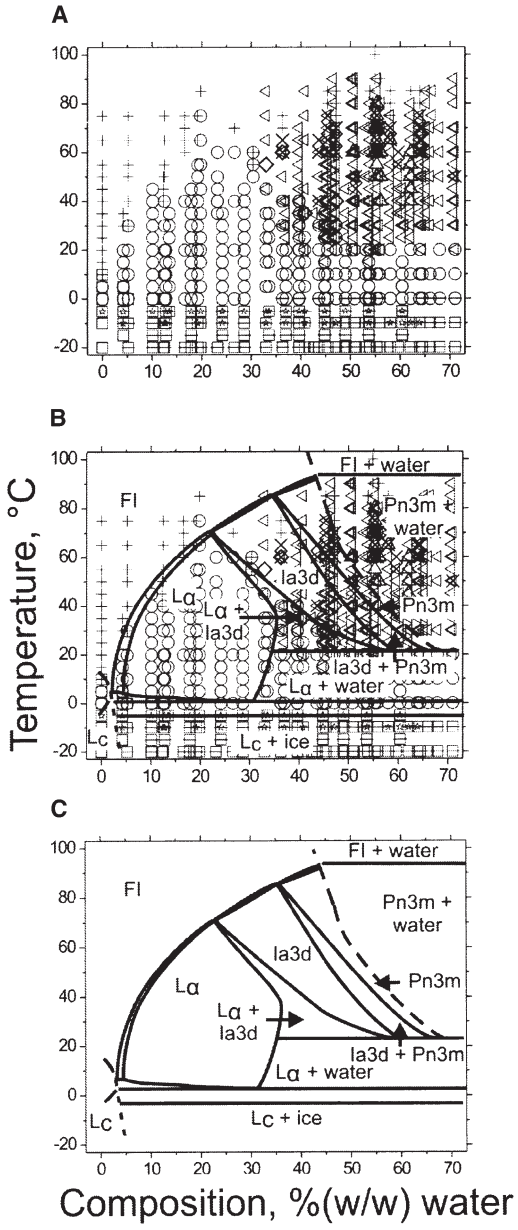

Figure 4. Temperature-Composition Phase Behavior of the 7.7 MAG/Water System Determined by X-Ray Diffraction in the Heating Direction

(A) The identity of the various phases in the 7.7 MAG/water system and their location in temperature-composition space. The identity of each of the phases is as follows: square, L_c; dash, ice; star, L_c* (L_c polymorph); circle, L_α; diamond, Cubic-Ia3d; triangle pointing up, Cubic-Pn3m; plus sign, Fl; multiplication sign, Single ring; triangle pointing to the left, Cubic.

(B) An overlay of the data in (A) with phase boundaries drawn in accordance with the Gibbs phase rule.

(C) Interpreted phase boundaries based on the data in (A) and on polarized light microscopy data from Supplemental Figure S2.

parameters: a = 45.4 Å, b = 103.3 Å, c = 104.3 Å, $\alpha = \beta = \gamma = 90°$) (Figure 7A) and showed no evidence of perfect merohedral twinning (Yeates, 1997). In contrast, the space group observed with 9.9 MAG was $P6_3$ (Luecke et al., 1998). A more complete analysis of these data will be reported on separately (V.C., Y.M., O.S., and M.C.; in preparation).

Crystallization trials of bR in 7.7 MAG and 9.9 MAG were also performed at 40°C; at this temperature, the cubic phase is fully developed in both lipid systems. Several screen solutions produced crystals in 9.9 MAG. However, none formed in the case of the short-chained lipid. Instead, the protein denatured as evidenced by a loss of its native pink/purplish color. Despite the denaturation, the lipid remained in the cubic phase.

Significantly, the colorless, outer membrane protein, BtuB, was crystallized in both the 7.7 and 9.9 MAGs at 20°C (Figures 6E and 6F). The crystals produced in 7.7 MAG were larger and of a better quality visually than those in 9.9 MAG. Fine screening in the latter system was followed by crystal harvesting, cryo-cooling, and diffraction data collection. The crystals diffracted to ~4 Å. They most likely belong to space group P222 with lattice parameters a = 149.6 Å, b = 157.3 Å, c = 82.0 Å, $\alpha = \beta = \gamma = 90°$ (Figure 7B). Further screening to grow better-quality crystals is in progress.

The cubic phase has been used to grow crystals of soluble proteins (see Caffrey, 2003, for example). The ability of 7.7 MAG to serve in this capacity was investigated accordingly. The results show that, just like the benchmark lipid 9.9 MAG, it too supports the crystallization of the water-soluble protein, lysozyme (Figures 6G and 6H).

Discussion

In Meso Crystallization

This study was performed to determine if a short-chained MAG could be used to crystallize membrane proteins by the in meso method. A second objective was to compare crystallogenesis in the short-chained lipid with that in its longer-chained counterpart. Using the rational design approach, 7.7 MAG was identified as the short-chained lipid with which to perform the evaluation. The results show convincingly that it supports the crystallization of two very different membrane proteins.

7.7 MAG-grown crystals of bR were quite large (max. 0.2 mm) and diffracted to 2.1 Å. Particularly striking was the finding that the crystals grew in a space group different from that obtained with the benchmark 9.9 MAG at 20°C. This result demonstrates, as expected, that crystal form is sensitive to the identity of the hosting lipid. While a structure has not been determined with crystals grown in the short-chained lipid, it is possible that the details of the molecular form will also be different. Should this be so, the new arrangement has the potential of revealing novel aspects of the protein's structure and, by extension, new insights into its function. This result highlights the advantages of being able to grow crystals in a variety of hosting lipids. Each gives rise to a distinctly different phase microstructure and phase propensity, which in turn allows for the protein to form an ordered lattice in ways that reflect the unique character of the host. As a result, the prospect exists that new facets of a protein's structure can be revealed in one lipidic host that are lost to disorder in another.

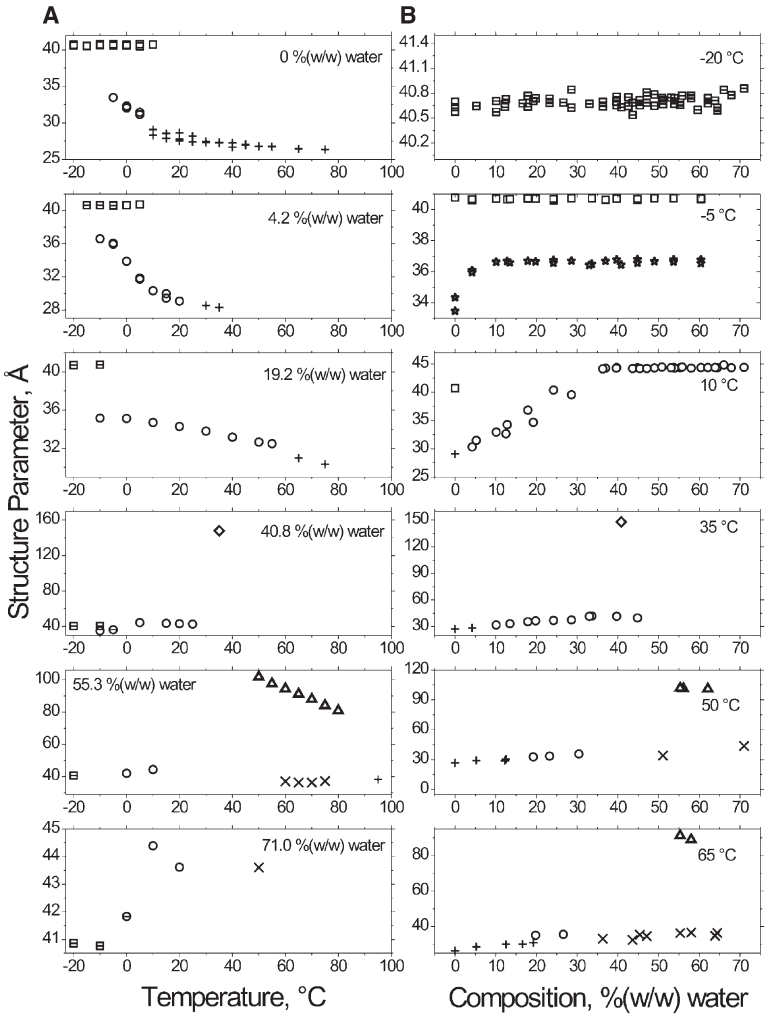

Figure 5. Structure Parameters of the 7.7 MAG/Water System Determined by X-Ray Diffraction

(A and B) The (A) temperature and (B) composition dependence of the structure parameters in the heating direction at the indicated sample compositions and temperatures. The identity of the phases is as follows: square, L_c; star, L_c* (L_c polymorph); circle, L_α; diamond, Cubic-Ia3d; triangle pointing up, Cubic-Pn3m; plus sign, FI; multiplication sign, Single ring. The coexistence of the Lc phase with ice is indicated by a dash superimposed on a square. The structure parameter values reported are accurate to $\pm$0.2 Å for the Lc and L_α phases and $\pm$3.0 Å for the cubic-Ia3d, cubic-Pn3m, FI, and single ring phases.

By using several lipids, full structural characterization is more likely.

In addition to bR, 7.7 MAG proved to be a useful host in which to grow crystals of the bacterial outer membrane protein, BtuB. This is a very significant result because it is the first example, to our knowledge, of an integral membrane β barrel protein to be crystallized by the in meso method. To date, all other successes have been with proteins that consist of relatively compact bundles of transmembranal helices stabilized by one or more chromophores. The fact that BtuB is colorless and produces crystals that can be seen and harvested for use in diffraction measurements also attests to the generality of the in meso method. Unfortunately, the BtuB crystals diffract weakly (~4 Å, Figure 7B). Refinement is in progress to produce better-quality crystals.

In addition to using the short-chained lipid for crystallization trials of membrane proteins, its ability to support soluble protein crystal growth was investigated. Crystals of the soluble protein, lysozyme, were found to grow equally well in the benchmark 9.9 MAG and in 7.7 MAG at 20°C. Since growth of soluble protein crystals is expected to occur in the aqueous compartment of the cubic phase, the chain identity of the MAG is not expected to impact dramatically on the process, as observed.

Phase Change during Crystallization

As has been reported (Misquitta and Caffrey, 2003), when a mixture of 9.9 MAG and bR is made under standard crystallization conditions, the initial phase is usually lamellar + cubic (usually cubic-Pn3m). Upon addition of a successful precipitant, like sodium/potassium phosphate, the lipidic phase is seen to change to the cubic-Pn3m phase (Misquitta and Caffrey, 2003), usually within an hour after a typical crystallization setup. In screens of BtuB in 9.9 MAG, the initial and final phases in successful screens were cubic. It is from the cubic phase that these proteins are observed to crystallize. And, the cubic phases in general have been proposed to be necessary for in meso crystallization of membrane proteins.

In the case of bR and BtuB at 20°C in 7.7 MAG, the phases seen are slightly different. The system started out as a mixture of the lamellar and cubic phases in 7.7 MAG/protein dispersion and evolved over time into an ill-defined fluid-like phase or a very disordered cubic phase that contained crystals. Thus, a phase transition

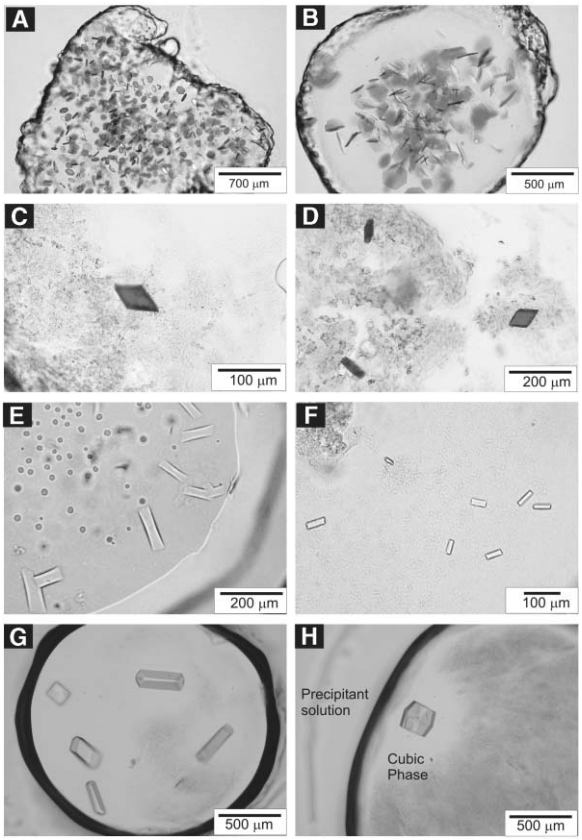

Figure 6. Crystals of Membrane and Soluble Proteins Grown In Meso

(A and B) Crystals of bR in 9.9 MAG.
(C and D) Crystals of bR in 7.7 MAG.
(E) Crystals of BtuB in 7.7 MAG.
(F) Crystals of BtuB in 9.9 MAG.
(G and H) Crystals of lysozyme in 7.7 MAG.
Length scales are included.

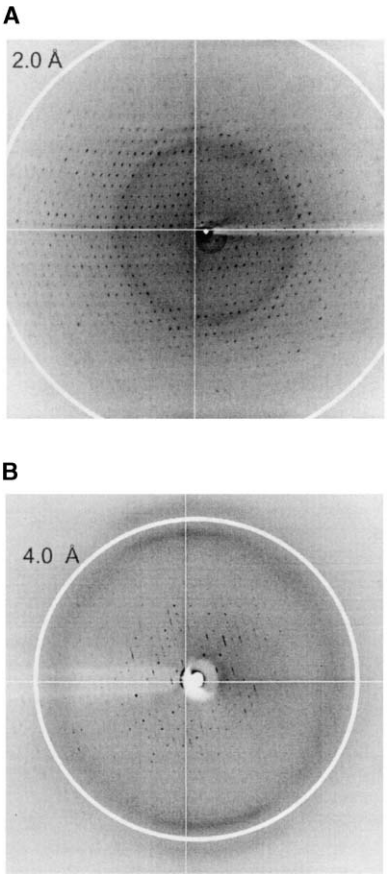

Figure 7. Diffraction Patterns of Membrane Proteins Grown in 7.7 MAG by the In Meso Method

(A) bR crystal (CHESS F1; λ, 0.919 Å; sample-to-detector distance, 200 mm; exposure, 30 s; oscillation, 1°).
(B) BtuB crystal (CHESS A1; λ, 0.976 Å; sample-to-detector distance, 250 mm; exposure, 90 s; oscillation, 1°). White rings at the resolutions indicated are included for reference.

occurred during the course of the incubation process. The precise time at which the "fluidization" took place after the screens were set up is not known. Nor indeed has the nature of the phase transformation been determined. This represents a work in progress. A similar "fluidization" phenomenon has been reported to occur during the crystallization of the acetylcholine receptor-α-bungarotoxin complex in the 9.9 MAG lipid system (Paas et al., 2003).

Protein Stability in the Cubic Phase

As seen in the temperature-composition phase diagram for 7.7 MAG (Figure 4C), the lamellar-to-cubic phase transition in excess water occurs at slightly above 20°C. In order to determine if bR could crystallize from a "well-developed" cubic phase of 7.7 MAG, crystallization trials were conducted at 40°C. Controls were run in parallel with 9.9 MAG at the same temperature. While several of the 9.9 MAG screens were successful at 40°C, none of the screens in 7.7 MAG grew at this temperature. Instead, the protein was found to have denatured, as indicated by a loss of color, even though the cubic phase was retained.

To what can we ascribe the stability difference of the bR protein in the cubic phase of the 7.7 and 9.9 MAGs? In what follows, we consider two properties of the respective hosts that relate to this question. The first is curvature. As will be shown below, the lipid/water interface of the cubic-Pn3m phase in hydrated 9.9 MAG is more highly curved than that of 7.7 MAG at the same temperature (40°C). The observation, that the protein denatures in the latter but not the former suggests that if curvature is an issue, then more (curvature) is better than less and a flatter membrane is more destabilizing. The other property is bilayer thickness. As seen in Figure 8, the two lipids differ in bilayer thickness by 6–7 Å. Thus, the mismatch between the hydrophobic surface of the protein and its complementary contacting surface in the bilayer interior is more pronounced in the shorter-chained MAG. The more-exposed apolar surface in the latter may contribute to the instability observed. The bilayer of the cubic phase thickens at lower temperatures (Caffrey, 2003). Presumably, it is thick enough to coat and to protect the protein at 20°C, since no sign of denaturation was observed under this condition with the short-chained lipid.

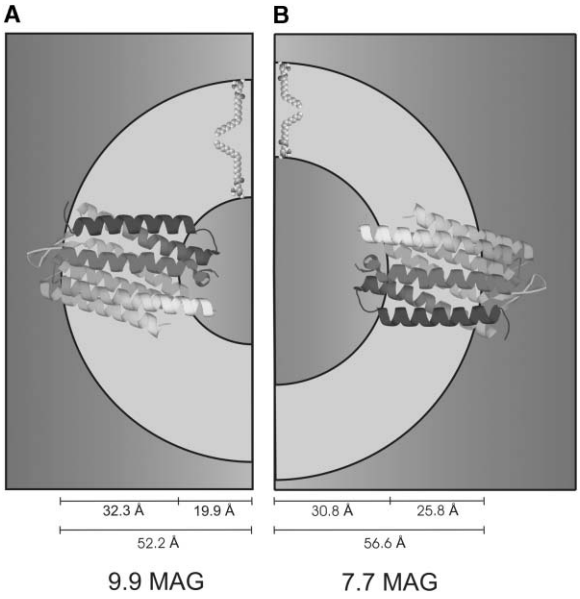

Figure 8. Cartoon Representation of bR in the Highly Curved Cubic Phase Bilayer of Fully Hydrated 7.7 MAG and 9.9 MAG at 40°C

The figure has been drawn to scale. It includes a ribbon diagram of bR (PDB ID: 1c3w). Dimensions shown were derived from X-ray diffraction measurements on fully hydrated lipid at 40°C (see text for details). The choice of orientation and relative position of the protein in the bilayer are described in the text.

Comparison of the Predicted and Experimental Phase Diagrams

Before embarking on a quantitative comparison of the predicted and experimentally determined phase diagrams for the 7.7 MAG/water system, it is important to recognize the magnitude of the uncertainties or errors associated with each. The experimental phase diagram (Figure 4C) is based on data collected at discrete values of temperature and composition in increments of 5°C and 2%–5% (w/w) water, respectively (Figure 6A). Phase boundaries were fit to these data by eye and have an estimated error of ±2.5°C and ±2.0% (w/w) water. We consider the assigned estimated errors of ±5°C and ±5% (w/w) water for the predicted phase diagram in Figures 3A and 3B to be conservative.

To facilitate the comparison, Figure 9 shows the experimental and the predicted diagrams side by side and as a superposition of one on the other. We have chosen not to examine the phase behavior at low temperatures at which the Lc phase dominates since it is the liquid crystal phases, and not the solid state, that are the focus of attention in this study.

A perusal of the data in Figure 9C shows that the predicted phases are all present in the experimental system, and that they are there in the expected relative positions with respect to temperature and composition. Thus, the L_α, cubic-Ia3d, cubic-Pn3m, and FI phase regions in the predicted and experimental diagrams overlap reasonably well considering the phase boundary errors noted. The 7.7 MAG system was not expected to form the H_{II} phase, which indeed is absent from the predicted phase diagram. This was borne out experimentally (Figure 9A).

Impact of Lipid Phase Microstructure on Crystallogenesis

During the early stages of this project, it was unclear that the target short-chained lipid, 7.7 MAG, would work as a host for the in meso crystallization of membrane proteins. To begin with, it was deemed necessary that the lipid form the cubic phase under conditions of full hydration at room temperature (Caffrey, 2000). The predicted phase behavior indicated that this might possibly be the case, and the experimental diagram verified it. The second issue was effective acyl chain length, and the possibility that the thickness of the bilayer of the cubic phase formed by this short-chained lipid would be too small to support an active transmembranal protein. While activity assays were not performed on the reconstituted proteins, the system went on to produce diffraction-quality crystals in the case of bR (Figures 6C and 6D). We are assuming therefore that the crystals incorporate the active form of the protein, as has been shown to exist for those grown with 9.9 MAG (Heberle et al., 1998).

While the 7.7 and 9.9 MAGs differ in acyl chain length by four methylenes, it is not necessarily true that the metrics of the bilayers constituting the assorted phases that they form will directly reflect this difference. However, a reasonably direct measure of this can be obtained from the phase microstructure characterization carried out in this study. It so happens that the Lc phase of both lipids forms with little or no associated water (Figure 4, and Figure 2 in Qiu and Caffrey [2000]). Accordingly, its lamellar spacing (d_{001}) approximates the thickness of the bilayer in the layered sheets that constitute this solid phase. For 7.7 MAG, the corresponding value is ~41 Å (Figure 5 and Supplemental Table S1). Each methylene in the *trans* configuration adds 1.25 Å to the width of a bilayer when the chain is oriented normal to the bilayer plane. Accordingly, this d_{001} value can be incremented by ($8 \times 1.25 =$) 10 Å, providing an expected value of 51 Å for the Lc phase of 9.9 MAG. The experimental value is 49.3 Å (Qiu and Caffrey, 2000), which is in reasonable agreement with the value just calculated. Given that the chains contain a *cis* olefinic group and are thus kinked, the slightly lower experimental value is not unreasonable.

For the cubic phase used in membrane protein crystallization, the microstructure comparison is not as straightforward as with the Lc phase. The complication arises because the measured lattice parameter has two components, lipid and water. The relative contributions of each can be obtained under certain limiting conditions. The hydration level at which the cubic phase saturates with water is one such limit that is commonly used. This, in turn, defines the composition of the phase at the specified temperature. Assuming that the lipid and water are equally dense, it is possible to calculate various parameters that describe the microstructure of the cubic phase, as has been outlined elsewhere (Briggs et al., 1996; Qiu and Caffrey, 1999). Since the cubic phase that is in equilibrium with excess water is of the Pn3m type for both the 7.7 and 9.9 MAGs, it is this that we will focus on for purposes of comparison. Further, the evaluation will be done at 40°C. This is the lowest common temperature for which indexable diffraction patterns for the cubic-Pn3m phase were obtained.

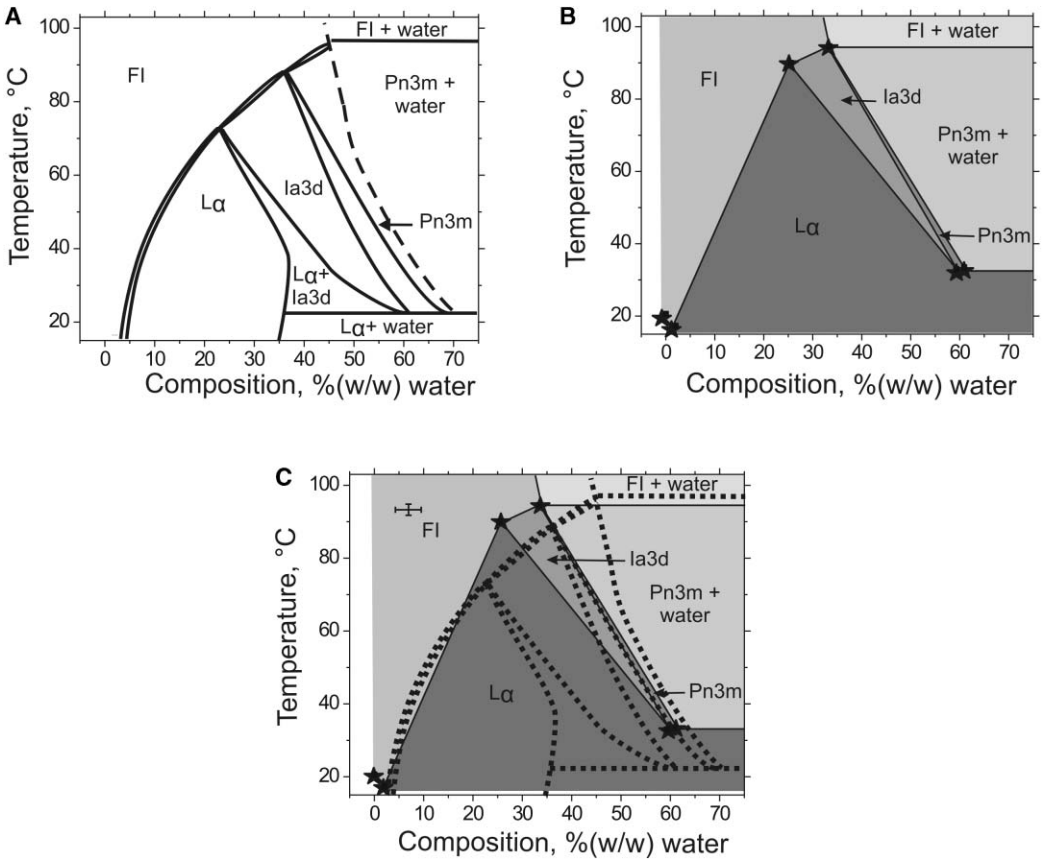

Figure 9. A Comparison of the Interpreted and the Predicted Phase Diagrams for the 7.7 MAG/Water System

(A) Interpreted phase diagram.

(B) Predicted phase diagram. (A) and (B) are taken from Figures 4 and 3, respectively.

(C) An overlay of (A) and (B), with the boundaries in (A) shown as dashed lines to facilitate comparison. The error bars shown are those associated with the predicted phase diagram.

The excess water boundary at 40°C is observed at 56.9% and 37.2% (w/w) water in the case of the 7.7 (Figure 4C) and 9.9 MAGs (Qiu and Caffrey, 2000), respectively. The lattice parameter of the cubic-Pn3m phase, *a*, at 40°C is 111.7 Å and 92.1 Å for the 7.7 and 9.9 MAGs, respectively (Supplemental Table S1). These translate into bilayer thickness, *2l*, values of 25.8 Å and 32.3 Å and water channel diameter, d_w, values of 61.5 and 39.7 Å, respectively (Figure 8) (Qiu and Caffrey, 1998).

Before considering these microstructure characteristics in the context of in meso crystallization, it is instructive to use them to provide a measure of lipid shape within the cubic phase. The shape factor or packing parameter, γ, is a simple and quantitative way of describing molecular shape in a self-assembled aggregate such as the assorted lyotropic liquid crystal phases encountered in lipidic systems. In the bicontinuous cubic phase, γ can be calculated based on the infinite periodic minimal surface model as follows:

$$\gamma = \frac{V}{A(l)l} = \frac{\phi_l a^3}{2l(A_0 a^2 + 2\pi\chi l^2)}, \quad (1)$$

where *V* is lipid molecular volume, *A(l)* is the lipid headgroup area, *l* is lipid length, ϕ_l is the volume fraction of lipid in the unit cell (approximated as the weight fraction of lipid in the sample based on the assumption that lipid and water density are equal), *a* is the cubic phase lattice parameter, A_0 is the dimensionless ratio of the minimal surface in the unit cell to the quantity (unit cell volume)$^{2/3}$, and χ is the Euler-Poincare characteristic. In the case of the cubic-Pn3m phase, $A_0 = 1.919$ and $\chi = -2$ (Briggs et al., 1996; Qiu and Caffrey, 1998). The values of γ calculated for the 7.7 and 9.9 MAGs at 40°C are 1.04 and 1.17, respectively.

The shape factor for 9.9 MAG is larger than that for 7.7 MAG, indicating that the longer-chained lipid has the more-pronounced wedge shape at a fixed temperature. As has been described (Briggs et al., 1996; Qiu, 1998), a larger γ indicates that the lipid/water interface is more highly curved, and by extension, that the cubic phase accommodates less water. The relative hydrations of the excess water boundaries of the cubic-Pn3m phase of the two MAGs at 40°C, indicated above, bear out this statement. The lamellar-to-cubic phase transition of 9.9 MAG is also lower than that of 7.7 MAG at all hydrations, as expected (Briggs et al., 1996; Qiu, 1998). This is important, as membrane curvature has been postulated to be a driving force for the crystalliza-

tion of membrane proteins by the in meso method (Caffrey, 2000; Nollert et al., 2001; Grabe et al., 2003), as noted.

A cartoon representation of bR in a section of bilayer from the highly curved cubic phase is shown in Figure 8. The drawing is to scale to illustrate the relationship between the protein and the bilayer it presumably traverses after reconstitution. Cartoons are shown for the 7.7 and 9.9 MAGs; in these cartoons, their contrasting microstructures are readily apparent when viewed with respect to one another and to bR. The particular protein orientation and relative position chosen for illustration are arbitrary other than to have the long helices cross the bilayer and for the interhelical loops and the N and C termini to be extramembranal. For purposes of this discussion, deformation of the lipid bilayer around the protein is not invoked. A perusal of the figure shows that the bulk of the protein is accommodated within the bilayer of 9.9 MAG. However, in 7.7 MAG, a significant fraction of the protein extends beyond it. Assuming the protein can be approximated by an ellipsoid measuring $\sim 25 \times 33 \times 52$ Å^3, a simple calculation shows that the surface area difference exposed upon going from 9.9 to 7.7 MAG is $\sim$750 Å^2. This assumes, of course, that the protein conformation and the degree of oligomerization and tilt within the membrane do not change in response to a shortening of the lipid chain. If the area were entirely hydrophobic, the energy cost of exposure to water would be considerable (0.2 kJ/(mol. Å^2); Tanford, 1973; Kellis et al., 1988). This may contribute to the pronounced instability of bR in 7.7 MAG at 40°C that was not seen with 9.9 MAG. In contrast, at 20°C, at which the protein is stable and goes on to produce crystals in the short-chained lipid, the bilayer thickens up, leaving less of the protein surface exposed.

Conclusions

We have shown that the short-chained lipid, 7.7 MAG, forms the cubic phase when fully hydrated and that it can be used for in meso crystallization at 20°C. Crystals of the membrane proteins, bR and BtuB, and of the soluble protein, lysozyme, were successfully grown from mesophases prepared by using 7.7 MAG. In the case of bR, the crystals were of diffraction quality and adopted a habit, which was sensitive to acyl chain identity. The latter feature will be used to our advantage in a more complete characterization of integral membrane protein structure.

This work demonstrates that the in meso method is versatile when it comes to crystallizing integral membrane proteins. BtuB is a β barrel, while bR consists of transmembranal helices. The latter has a chromophore, while BtuB, at least the form used in this study, is devoid of potentially stabilizing cofactors. The fact that BtuB is colorless, but that it still can be worked with by the in meso method, should allay fears that the method is limited to colored proteins.

Membrane protein stability issues were addressed in this work. It was found that bR in the short-chained 7.7 MAG, while stable when reconstituted into the cubic phase at room temperature, denatured in the same phase at 40°C. In contrast, the protein was stable and produced crystals in the same cubic phase formed by the longer-chained 9.9 MAG at both temperatures. Given that bilayers become thinner with increasing temperature, these results suggest that a membrane can be too thin to support the native form of a protein, as in the case of bR in 7.7 MAG at 40°C. Thus, while working with the shorter-chained lipids may offer advantages, care is needed to ensure that there is a good match between the protein and the hosting lipid bilayer. Of course, the match is likely to be protein specific.

A related aim of this study was to examine the predictive power of a restricted database of phase diagrams for MAG/water systems. The intent was to use the set to identify a short-chained MAG that formed the cubic phase under standard in meso crystallization conditions. 7.7 MAG was identified and was shown to perform as expected. The prediction was based on the assumption that thermotropic and lyotropic phase behavior changes linearly with chain length. Despite the relatively coarse nature of the rational design approach, it did work.

Experimental Procedures

Materials

Racemic 7.7 MAG was synthesized and purified, as described by Coleman et al. (2004). bR was prepared in-house, as described by Dencher and Heyn (1982) and was used as a solution with ~20 mg protein/ml and a residual detergent concentration of 0.3 M octylglucoside (OG), estimated as described by Misquitta and Caffrey (2003). The *E. coli* outer membrane vitamin B_{12} receptor, BtuB, was expressed in *E. coli* strain TNEO12 (pJC3) and was purified as described by Taylor et al. (1998) and Kurisu et al. (2003), by using 1.5% OG for extraction and 0.1% LDAO during purification. The BtuB solution used for crystallization had a protein concentration of 7.5 mg/ml in 0.1 M NaCl, 0.1%(w/v) LDAO, 10 mM Tris (pH 8.0) buffer. Lysozyme was purchased from Sigma and was used as a 70 mg protein/ml solution in 0.1 M acetate buffer (pH 4.8).

Methods

Sample Preparation

Hydrated lipid samples were prepared at room temperature (between 19°C and 25°C) by using a home-built mechanical syringe mixer (Cheng et al., 1998; Qiu and Caffrey, 1998). Samples were loaded into 1 mm diameter capillaries (Hampton Research). The water content of each sample was determined gravimetrically (Cheng et al., 1998; Misquitta and Caffrey, 2001). The capillaries were flame sealed and glued with "5 minute" epoxy. Samples were stored at −70°C when the initial diffraction measurement was to be made at −20°C, and at 20°C, for a period of less than 1 day, when measurements started at 20°C.

Sample purity was determined by means of TLC after completing the diffraction experiment. The samples were found to contain at least 99% MAG.

X-Ray Diffraction

Mesophase powder diffraction experiments were performed by using nickel-filtered copper Kα X-rays (1.542 Å) from a rotating anode generator, as described by Cherezov et al. (2002).

For most MAG/water systems, incubation at −15°C enables the sample to access the assumed equilibrium Lc state (Qiu and Caffrey, 1999, 2000). This was not the case with 7.7 MAG, where it was found to be necessary to store the sample at −70°C for a period never exceeding 2 days for Lc formation. The capillaries were then transferred rapidly to a prechilled beryllium holder at −70°C and were incubated at −20°C for 3 hr or longer before data collection. They were then heated to the required temperature and incubated there for anywhere from 3 to 6 hr, at which point the diffraction pattern was collected by using an exposure time of 30–60 min per sample. This cycle of adjusting temperature followed by an incubation period

was repeated up to a temperature of 100°C. The 3–6 hr incubation period has been shown by relaxation experiments with 10.9 MAG to be sufficient for the sample to attain a phase of stable lattice parameter (Misquitta and Caffrey, 2001).

Diffraction patterns were recorded on image plates and were processed as described by Misquitta and Caffrey (2001).

Diffraction from bR crystals was recorded at the Cornell High Energy Synchrotron Source (CHESS) beamlines F1 (0.919 Å) and A1 (0.976 Å) with an ADSC Quantum 4 CCD detector (F1) and an ADSC Quantum 210 CCD detector (A1). Measurements were made with a 0.1 mm diameter beam in a liquid nitrogen-generated cryo-stream.

Crystallization

In meso crystallization was performed with either 7.7 MAG or 9.9 MAG as the lipid, and with lysozyme, bR, and BtuB as test proteins. The lipidic mesophase laden with protein was prepared as a 1/1 by volume mixture of lipid and protein solution and was dispensed into home-made 96-well crystallization plates by using a home-built in meso crystallization robot (Cherezov et al., 2004). A complete description of the sample preparation and dispensing procedure has been presented by Cheng et al. (1998), Misquitta and Caffrey (2003), and Cherezov et al. (2004). Trials were performed with 50 nl protein/lipid dispersion and 1 μl precipitant solution. Plates were incubated in the dark at 20°C (lysozyme, bR, BtuB) and at 40°C (lysozyme, bR) for up to 24 days. Crystallization was monitored by light microscopy, as described by Cherezov and Caffrey (2003) and Cherezov et al. (2004). Successful crystallization conditions for the membrane proteins are given in Supplemental Table S2.

Crystals of bR and BtuB for harvesting and diffraction measurement were grown in a 72-well Nunc microbatch plate (HR3-122, Hampton Research). 200 nl lipid/protein dispersion was used in each well in conjunction with 3 μl precipitant solution. Crystals were harvested with 0.1–0.2 mm mounted cryoloops (HR4-955, Hampton Research).

Supplemental Data

Supplemental Data including low- and wide-angle X-ray diffraction patterns, PLM images, phase lattice parameters, and crystallization conditions are available at http://www.structure.org/cgi/content/full/12/12/2113/DC1/.

Acknowledgments

M.C. thanks J. Clogston and L. Muthusubramaniam for invaluable input on this work. Grant support for M.C. was provided in part by the National Institutes of Health (NIH) (GM56969, GM61070), the National Science Foundation (DIR9016683, DBI9981990, IIS-0308078), and Science Foundation Ireland, and grant support for W.A.C. was provided by NIH GM-18457.

Received: August 23, 2004
Revised: September 24, 2004
Accepted: September 24, 2004
Published: December 7, 2004

References

Bailey, A.E. (1950). Melting and Solidification of Fats (New York: Interscience Publishers, Inc.).

Briggs, J. (1994). The phase behavior of hydrated monoacylglycerols and the design of an X-ray compatible scanning calorimeter. PhD thesis, The Ohio State University, Columbus, Ohio.

Briggs, J., and Caffrey, M. (1994a). The temperature-composition phase diagram and mesophase structure characterization of monopentadecenoin in water. Biophys. J. *67*, 1594–1602.

Briggs, J., and Caffrey, M. (1994b). The temperature-composition phase diagram of monomyristolein in water: equilibrium and metastability aspects. Biophys. J. *66*, 573–587.

Briggs, J., Chung, H., and Caffrey, M. (1996). The temperature-composition phase diagram and mesophase structure characterization of the monoolein/water system. J. Phys. II France *6*, 723–751.

Caffrey, M. (2000). A lipid's eye view of membrane protein crystallization in mesophases. Curr. Opin. Struct. Biol. *10*, 486–497.

Caffrey, M. (2003). Membrane protein crystallization. J. Struct. Biol. *124*, 108–132.

Cheng, A., Hummel, B., Qiu, H., and Caffrey, M. (1998). A simple mechanical mixer for small viscous samples. Chem. Phys. Lipids *95*, 11–21.

Cherezov, V., Qui, H., Pector, V., Vandenbranden, M., Ruysschaert, J.M., and Caffrey, M. (2002). Biophysical and transfection studies of the diC14-amidine/DNA complex. Biophys. J. *82*, 3105–3117.

Cherezov, V., and Caffrey, M. (2003). Nano-volume plates with excellent optical properties for fast, inexpensive crystallization screening of membrane proteins. J. Appl. Crystallogr. *36*, 1372–1377.

Cherezov, V., Peddi, A., Muthusubramaniam, L., Zheng, Y., and Caffrey, M. (2004). A robotic system for crystallizing membrane and soluble proteins in lipidic mesophases. Acta Crystallogr. D Biol. Crystallogr. *60*, 1795–1807.

Chimento, D.P., Mohanty, A.K., Kadner, R.J., and Wiener, M.C. (2003). Substrate-induced transmembrane signaling in the cobalamin transporter BtuB. Nat. Struct. Biol. *10*, 394–401.

Chiu, M.L., Nollert, P., Loewen, M.C., Belrhari, H., Pebay-Peyroula, E., Rosenbusch, J.P., and Landau, E.M. (2000). Crystallization in cubo: general applicability to membrane proteins. Acta Crystallogr. D Biol. Crystallogr. *56*, 781–784.

Chung, H., and Caffrey, M. (1995). Polymorphism, mesomorphism, and metastability of monoelaidin in excess water. Biophys. J. *69*, 1951–1963.

Coleman, B.E., Cwynar, V., Hart, D.J., Havas, F., Mohan, J.M., Patterson, S., Ridenour, S., Schmidt, M., Smith, E., and Wells, A.J. (2004). Modular approach to the synthesis of unsaturated 1-monoacyl glycerols. Synlett *8*, 1339–1342.

Dencher, N.A., and Heyn, M.P. (1982). Preparation and properties of monomeric bacteriorhodopsin. Methods Enzymol. *88*, 5–10.

Gordeliy, V.I., Labahn, J., Moukhametzianov, R., Efremov, R., Granzin, J., Schlesinger, R., Buldt, G., Savopol, T., Scheidig, A.J., Klare, J.P., et al. (2002). Molecular basis of transmembrane signaling by sensory rhodopsin II-transducer complex. Nature *419*, 484–487.

Grabe, M., Neu, J., Nollert, P., and Oster, G. (2003). Protein interactions and membrane geometry. Biophys. J. *84*, 854–888.

Heberle, J., Buldt, G., Koglin, E., Rosenbusch, J.P., and Landau, E.M. (1998). Assessing the functionality of a membrane protein in a three-dimensional crystal. J. Mol. Biol. *281*, 587–592.

Katona, G., Andreasson, U., Landau, E.M., Andreasson, L.E., and Neutze, R. (2003). Lipidic cubic phase crystal structure of the photosynthetic reaction centre from *Rhodobacter sphaeroides* at 2.35 Å resolution. J. Mol. Biol. *331*, 681–692.

Kellis, J.T., Nyberg, K., Sali, D., and Fersht, A.R. (1988). Contribution of hydrophobic interactions to protein stability. Nature *333*, 784–786.

Kolbe, M., Besir, H., Essen, L.O., and Oesterhelt, D. (2000). Structure of the light driven chloride pump halorhodopsin at 1.8 Å resolution. Science *288*, 1390–1396.

Kurisu, G., Zakharov, S.D., Zhalnina, M.V., Bano, S., Eroukova, V.Y., Rokitskaya, T.I., Antonenko, Y.N., Wiener, M.C., and Cramer, W.A. (2003). The structure of BtuB with bound colicin E3 R-domain implies a translocon. Nat. Struct. Biol. *10*, 948–954.

Landau, E.M., and Rosenbusch, J.P. (1996). Lipidic cubic phases: a novel concept for the crystallization of membrane proteins. Proc. Natl. Acad. Sci. USA *93*, 14532–14535.

Lanyi, J.K., and Schobert, B. (2004). Local-Global conformation coupling in a heptahelical membrane protein: transport mechanism from crystal structures of the nine states in the bacteriorhodopsin photocycle. Biochemistry *43*, 3–8.

Luecke, H., Richter, H.T., and Lanyi, J.K. (1998). Proton transfer pathway in bacteriorhodopsin at 2.3 Å resolution. Science *280*, 1934–1937.

Luecke, H., Schobert, B., Lanyi, J.K., Spudich, E.N., and Spudich, J.L. (2001). Crystal structure of sensory rhodopsin II at 2.4 Å: insights into color tuning and transducer interaction. Science *293*, 1499–1503.

Lutton, E.S. (1965). Phase behavior of aqueous systems of monoglycerides. J. Am. Oil Chem. Soc. *42*, 1068–1070.

Misquitta, Y., and Caffrey, M. (2001). Rational design of lipid molecular structure: a case study involving the C19:1c10 monoacylglycerol. Biophys. J. *81*, 1047–1058.

Misquitta, Y., and Caffrey, M. (2003). Detergents destabilize the cubic phase of monoolein. Implications for membrane protein crystallization. Biophys. J. *85*, 3084–3096.

Misquitta, Y., Cherezov, V., Havas, F., Patterson, S., Mohan, J.M., Wells, A.J., Hart, D.J., and Caffrey, M. (2004). Rational design of lipid for membrane protein crystallization. J. Struct. Biol., *148*, 169–175.

Nollert, P., Qiu, H., Caffrey, M., Rosenbusch, J.P., and Landau, E.M. (2001). Molecular mechanism for the crystallization of bacteriorhodopsin in lipidic cubic phases. FEBS Lett. *504*, 179–186.

Paas, Y., Cartaud, J., Recouvreur, M., Grailhe, R., Dufresne, V., Pebay-Peyroula, E., Landau, E.M., and Changeux, J. (2003). Electron microscopic evidence for nucleation and growth of 3D acetylcholine receptor microcrystals in structured lipid-detergent matrices. Proc. Natl. Acad. Sci. USA *100*, 11309–11314.

Qiu, H. (1998). The mesophase behavior of the monoacylglycerol/water systems; application in drug delivery. PhD thesis, The Ohio State University, Columbus, Ohio.

Qiu, H., and Caffrey, M. (1998). Lyotropic and thermotropic phase behavior of hydrated monoacylglycerols: structure characterization of monovaccenin. J. Phys. Chem. B *102*, 4819–4829.

Qiu, H., and Caffrey, M. (1999). Phase behavior of the monoerucin/water system. Chem. Phys. Lipids *100*, 55–79.

Qiu, H., and Caffrey, M. (2000). Phase properties of the monoolein/water system: metastability and equilibrium aspects. Biomaterials *21*, 223–234.

Schobert, B., Cupp-Vickery, J., Hornak, V., Smith, S.O., and Lanyi, J.K. (2002). Crystallographic structure of the K intermediate of bacteriorhodopsin: conservation of free energy after photoisomerization of the retinal. J. Mol. Biol. *321*, 715–726.

Stowell, M.H., McPhillips, T.M., Rees, D.C., Soltis, S.M., Abresch, E., and Feher, G. (1997). Light-induced structural changes in photosynthetic reaction center: implications for mechanism of electron-proton transfer. Science *276*, 812–816.

Tanford, C. (1973). The Hydrophobic Effect: Formation of Micelles and Biological Membranes (New York: John Wiley & Sons).

Taylor, R., Burgner, J.W., Clifton, J., and Cramer, W.A. (1998). Purification and characterization of monomeric *Escherichia coli* vitamin B_{12} receptor with high affinity for colicin E3. J. Biol. Chem. *273*, 31113–31118.

Yeates, T.O. (1997). Detecting and overcoming crystal twinning. Methods Enzymol. *276*, 344–358.